Bar-Ilan University

Department of Physics

Abrupt Phase-Transitions in Interdependent Superconducting Networks

Maayan Laav

Submitted in partial fulfillment of the requirement for the Master's Degree in the Department of Physics,

Bar-Ilan University

Ramat-Gan, Israel October, 2021

This work was carried out under the supervision of Prof. Aviad Frydman of the Department of Physics, Bar-Ilan University

Acknowledgements

I would like to express my deep gratitude to Dr. Irina Volotsenko, my lab manager, for supporting me throughout the research, from depositing samples to assisting with measurements. This work could not be done without your help.

In addition, I would like to thank our collaborators, Bnaya Gross, Dr. Ivam Bonamess and Prof. Shlomo Havlin, for all the hard work and perseverance in developing a theory for our experiment.

I would like to thank my fellow lab members, past and present: Avital Fried, Dr. Arnab Roy, Dr. Gopi Nath Daptary, Idan Cohen, Mark Nikolaevsky, Moshe Haim, Roy Cohen, Yehudit Stein and Yuxiao Wu.

I would like to take this opportunity and thank my parents, Liat and Eli Laav for pushing me ever-forward and providing me with everything I needed to get here. Thank you for inspiring curiosity. I hope this will make you proud.

Last and most importantly, I would like thank from the bottom of my heart to my supervisor, Prof. Aviad Frydman, for giving me the opportunity to carry this research under his guidance. Thank you for setting challenges, inspiring passion to the subject, and for pushing me in the right direction.

Table of Contents

Abstract

In nature, networks rarely appear in isolation. They are typically elements in larger systems and can have non-trivial effects on one another. In the light of this situation the model of interdependent networks (i.e. systems where the functionality of a node in one layer depends on the functionality of other nodes in the remaining ones) was developed. In particular, after a seminal article [1], increasing evidence has been collected showing that interdependent networks exhibit *unique phenomena* resulting in abrupt transitions. A striking example is the famous 2003 Italy blackout.

Although the model of interdependent network has been studied more than a decade, it has never been applied on real-world physical system. Our study, is the first attempt to do this. For this purpose, we coupled two disordered superconducting networks via a medium that is an electrical insulator but a heat conductor. Because of the disorder, each node in a network has its own critical temperature and critical current (T_c, I_c), thus, we can control the functionality of nodes in the networks. The coupling between the networks is created by passing the same current within both networks simultaneously, thus generating links based on heat-transfer between the networks.

We preformed Resistance vs Temperature measurements of both networks simultaneously and each network separately for different currents. Our main result is that the RT curves of both coupled networks for a certain current exhibit an abrupt transition and hysteretic behaviour with a shared T_c, while the RT curve of each uncoupled network for the same current exhibit a continuous transition with a different T_c in each network. The shared T_c is determined by T_c of the network with the lower transition temperature.

We collaborated with Prof. Shlomo Havlin's group and developed a theory based on random network of Josephson Junctions that can explained our results.

We trust that our experimental results, together with the simulation results of Havlin Group's will pave the way to engineer interdependent physical processes, whose achievement may lead to new technological applications such as ultra-sensitive sensors.

1 Theoretical Background

1.1 Network percolation theory

There are only a few available theoretical techniques for dealing with flow in disordered, random and complex systems. One of the nicest and simplest of these techniques is the percolation theory. A manifestation of this theory deals with a model of a random graph, in which the bonds between each two neighboring nodes may be *open* with probability p or *closed* with probability $1 - p$. Adjacent opened bonds are considered as clusters, and each bond state is independent of the state of its adjacent bonds. The main research question of this model is what critical fraction of bonds must be *open* in order to connect the edges of the graph, this critical fraction is called the percolation threshold and marked as p_c.

A simple physical example for the percolation model can be the electrical-network. This model describes a network represented by a large 2D square-lattice of unit conductors that is attacked by a crazed man who, armed with a wire-cutter, proceeds to cut the unit conductors at random as illustrated in Fig. 1. His aim is to break the connectivity in the network. In this case the main question is: what critical fraction of bonds (unit conductors) must remain un-cut in order for the electrical network to still be connected. This question, of which can be given a definite answer by percolation theory, illustrates the most significant issue of the percolation model: the existence of percolation-transition at which the long-range connectivity of the system disappears or, for reasons of symmetry, appears. This basic transition, which occurs abruptly, constitutes p_c.

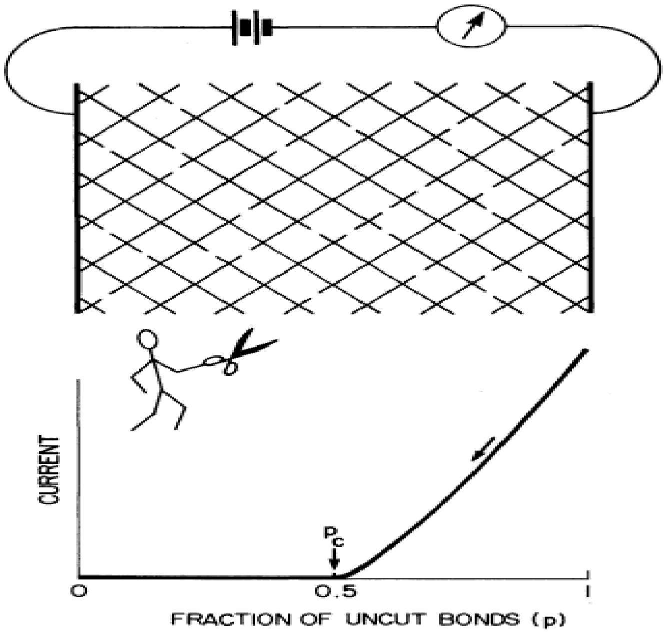

Figure 1: Top - electrical circuit that contains resistors network as one of its components.
Bottom - The current within the network as a function of uncut bonds (p). When p is larger than $\boldsymbol{p_c}$, current is still flowing and there is connectivity in the system. When p is less than $\boldsymbol{p_c}$ current vanishes since there is no connected path of unit conductors that traverses the network from one side to other [2].

One of the main parameters of percolation theory is the percolation probability ($P(p)$ or P_∞). It describes the probability to randomly choose a bond from the entire system that is connected to a cluster that traverses the network. Fig. 2 illustrates the behavior of $P(p)$ in a 2D percolation.

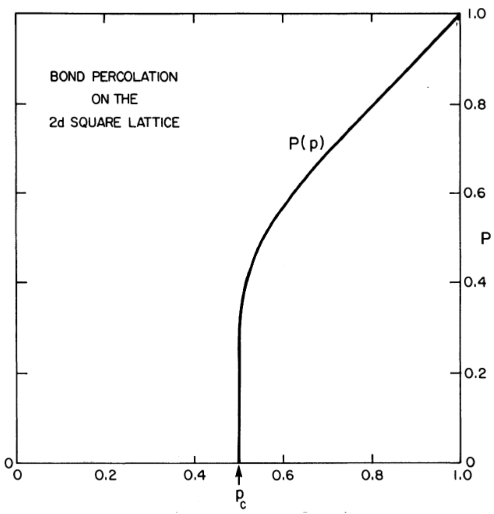

Figure 2: $P(p)$ as a function of connected bonds, p [3].

$P(p)$ shows the qualitative change at p_c as long-range connectivity transfers from zero where the network is disconnected to a finite value where a cluster that traverses the network first appears. It was found out that close to the threshold, the behavior of $P(p)$ is universal (independent on the network and type of interactions) and can be described by critical exponent ($P(p) \propto (p - p_c)^{\beta}$). The qualitative shape and the universality of $P(p)$ indicates that the system undergoes a second order phase transition, $P(p)$ being the order parameter which drops to zero rapidly but continuously as p_c is approached.

Another property of network percolation theory which is important for our research is the existence of the Giant Connected Component (GCC), which contains all the nodes that are connected to the cluster that traverses the network.

1.2 Interdependent networks

Single network percolation theory has been extensively developed and studied for a wide range of fields over the past few decades [4–10]. It was realized recently that many real-world systems include macroscopic subsystems which influence one another. Taking into account the mesoscopic organization of these interwoven structures has led to the understanding that interactions among systems can significantly modify the collective behaviors of processes acting on them, leading to a phenomenology that is unexpected if one considers the same systems in isolation [11–13]. One of the most interesting models describing an interacting complex system is the interdependent network model developed by our collaborator Prof. Shlomo Havlin [14]. This model describes a system of connected networks that exhibits cascading failures and explosive collective phenomena resulting in abrupt phase transitions. Remarkably, though being discontinuous and irreversible, these novel transitions display also critical scaling and are hence susceptible to universal features, whose study is in its infancy [15–17].

The distinctive feature of the interdependent networks model is the existence of two types of links which represent two qualitatively different kinds of interactions. Within networks, links between nodes describe *connectivity* in the sense that physical process (e.g., electric current) can spread through the network, moving from one node to another. Between networks, on the other hand, links describe *dependency* relationships which cause dependent nodes to crucially influence each other, without letting the physical processes within each network hop to the other. The outcome of distinguishing between dependency and connectivity links becomes transparent when considering a percolation process to describe the system stability against the failure of some of its components. In contrast with isolated systems, where the existence of at least one path that connects any randomly chosen node in the network to the GCC can be adopted as a proxy for functionality, in the presence of interdependencies the functionality of nodes is stricter. Even if a node is connected to the GCC, it will cease to function if the nodes upon which it depends on will cease to function. Therefore, while the connectivity links physically spread the damage within the networks, the dependency links spread instantaneously the information about local malfunctions across the networks.

The interplay between these two types of links amplifies the propagation of failures which, in its turn, can ignite percolation cascades and lead to an abrupt collapse of the system. A generalization of percolation theory to interdependent networks was developed in Ref. [14] and was able to explain the famous 2003 Italy blackout (see Fig. 3).

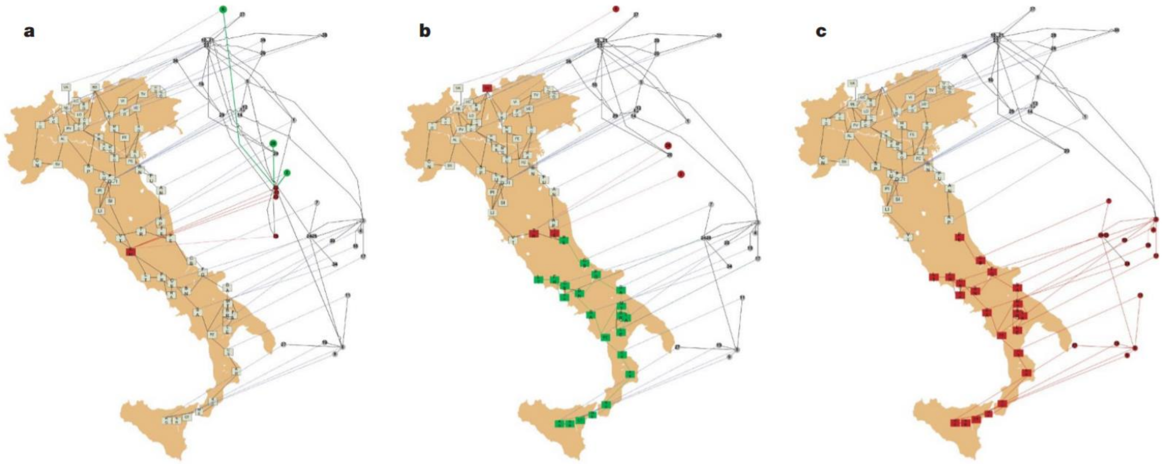

Figure 3: Illustration of an iterative process of the propagation of the famous 2003 Italy blackout using real-world data from a power network (located on the map of Italy) and an internet network (shift above the map). **a** - One power station is removed (red node on map) from the power network and as a result the Internet nodes depending on it are removed from the Internet network (red nodes above the map). The nodes that will be disconnected from the giant cluster (a cluster that spans the entire network) at the next step are marked in green. **b** - Additional nodes that were disconnected from the Internet communication network giant component are removed (red nodes above map). As a result, the power stations depending on them are removed from the power network (red nodes on map). Again, the nodes that will be disconnected from the giant cluster at the next step are marked in green. **c** - Additional nodes that were disconnected from the giant component of the power network are removed (red nodes on map) as well as the nodes in the Internet network that depend on them (red nodes above map).

It was found that, the mutual GCC (the MGCC, i.e., the set of nodes defined to be functional in the presence of interdependent links) can suddenly vanish by undergoing a unique first order phase transition at a finite critical threshold, characterized a discontinuous and abrupt jump (see Fig. 4), while simultaneously hosting critical phenomena. These results illustrate the fundamental uniqueness of an interdependent network system, the occurrence of a first order phase transition instead of second order when the networks are in isolation.

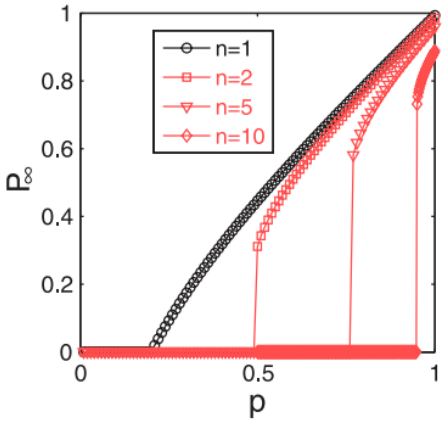

Figure 4: The percolation probability as a function of the fraction of connected nodes in interdependent random networks. n is the number of interdependent networks.

Although there are many implications in various network realizations of this model, it has never been reproduced in real physical systems.

1.3 Random resistor networks

Transport in disordered media is a classic problem in statistical physics which attracts much attention due to its broad range of applications. Examples include flow through porous material and conductivity of semiconducting materials or systems that undergo a metal-insulator transition. These problems have been mainly studied using a random resistor network, RRN, model with bonds that have a resistance chosen from a probability distribution mimicking the nature of the physical problem under consideration. Using this model, Kirkpatrick and others [18-20] demonstrated that percolation on diluted d-dimensional lattices has a rich phenomenology that can be adopted to explain conductivity in disordered media [21-23]. An important result that emerged from the study of isolated resistor networks was that the conductivity of the system and the GCC undergo a continuous phase transition at certain p_c [24]. ‘

1.4 Interdependent random resistor networks

The RRN can be extended to interdependent random resistor networks. Recently, a theoretical analysis of a system of two interdependent resistor networks has been carried out [25], showing that this system exhibits explosive collective behaviors resulting in first order phase transition. In these simulations, interdependent couplings are taken to represent interactions between current flows. Hence, a node in one layer can be considered as functional if and only if there is current flowing through it and also through the node that it depends on in the other network. Fig. 5 shows the main result of the simulations.

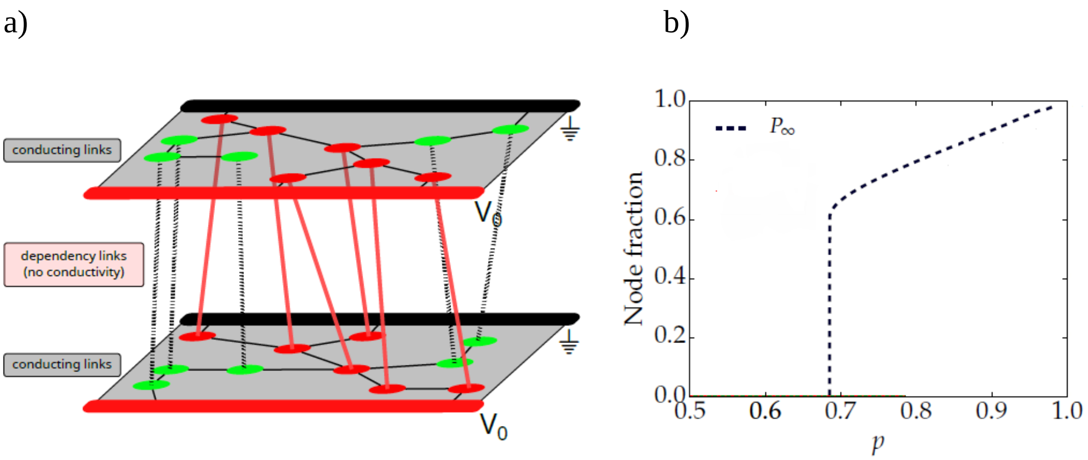

Figure 5: **a)** Sketch of the model - the red nodes have current flowing through them, whilst green ones do not. Note that the currents flow only through electrical connection within each layer, but cannot flow from one layer to another. **b)** the MGCC as a function of active nodes in the system.

It is seen that the MGCC undergoes an abrupt, discontinuous first order phase transition, in contrast to the second order transition obtained in a single RRN.

1.5 Superconductivity and disordered superconductors

In our work we use disordered superconductors in order to apply interdependent networks to a real physical system. The phenomenon of superconductivity is well understood in a perfect crystal (i.e., in the absence of impurities) thanks to the work of Bardeen, Schrieffer, and Cooper (BCS) [26]. Anderson extended the theory and predicted that superconductivity can exist even in weakly disordered superconductors with non-magnetic impurities [27]. However, experiments showed that for strong enough disordered thin films the system transits into an insulator state [28-31], in what has been called the superconductor insulator transition (SIT). Experimentally a wide variety of tuning parameters, g, was used for the SIT, including thickness, magnetic field, disorder level, chemical structure, etc. [29, 31-32, 33-40].

An example for an SIT can be seen in Fig. 6 that presents transport measurements in a sample of an amorphous indium oxide (a-InO) film driven continuously through a disorder-induced SIT. Changing the disorder level is achieved by low-temperature thermal annealing.

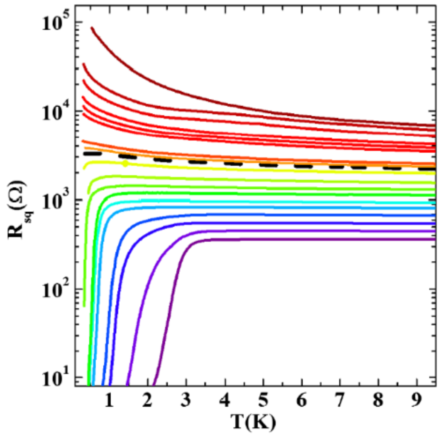

Figure 6: $R_{\square}$ versus T of an a-InO film for different annealing stages. The dashed line curve separates the insulating and superconducting stages. Taken from [41].

In these highly disordered superconductors [42] it has been established that they may have regions with different normal state resistance (R_N), critical temperature (T_c) and critical current (I_c). Fig. 7 demonstrates the spatial distribution of the superconducting energy gap, Δ, on a disordered superconductor pointing through inhomogeneities in T_c.

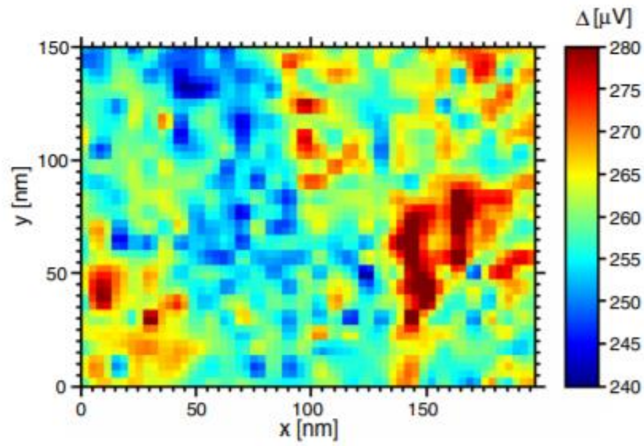

Figure 7: Spatial fluctuations of the superconducting gap, Δ, in thin films of TiN, a disordered superconductor. Inhomogeneities in Δ are seen on a scale of a few tens of nanometers [42].

2 Motivation and Potential Outcome

Our research is the first attempt to create a real-world physical system of interdependent resistors networks and to understand the physical mechanism of dependency interactions in a solid-state device. This is done by developing a system of disordered superconducting networks coupled by a heat conducting medium, measuring it and analyzing the critical phenomena around T_c.

As described in the theoretical background section, systems of interdependent networks must contain two different kinds of interactions (see Fig. 8):

a. *Connectivity interactions* - interactions between nodes in the same network.

b. *Dependency interaction*s - crossing interactions between dependent nodes.

In our system, the current passing through the networks acts as the connectivity links and heat that flows between the networks, via a heat conducting medium, serves as the dependency links. The medium is an electrical insulator separating the two conducting networks.

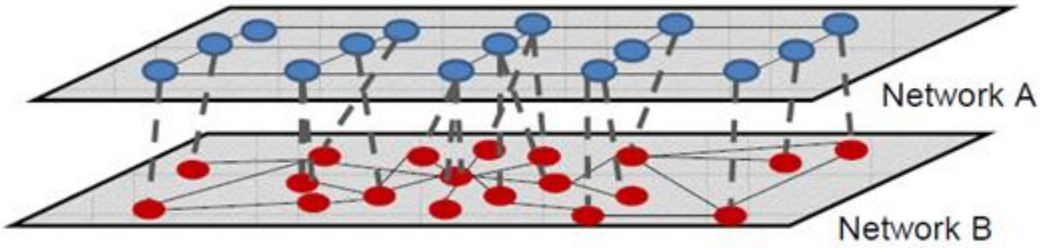

Figure 8: Sketch of the interdependent resistor networks. Current can flow through blue nodes in network A and red nodes in B. In addition, there are dependency links between the networks.

Our experimental idea is based on the fact that, because of the disorder, each network link undergoes a metal-superconductor transition at a different critical temperature, T_c and different critical current, I_c.

We initiate the system at low temperatures to ensure that all the links are in the superconductor phase, and then we adiabatically increase the heat-bath temperature close to the average critical temperature T_c. Consequently, some superconducting links randomly switch to a normal metal phase, thus causing a dissipative current flow and heating. Due to thermal coupling, this local temperature increases and heats the superposed links in the other layer, heating in turn an increasingly growing number of links. This feedback thermal process continues while developing a voltage across the network, leading to a cascade of failures and a first-order phase transition.

The main outcome of this project is likely to have a scientific and economic impact with the high gain of creating brand new generations of complexity-based material. In fact, besides being effective in unveiling the underlying mechanisms of these novel phase transitions whose importance is indeed interdisciplinary, we created the very first prototype of an interdependent complex system by physically realizing interdependent interactions between systems in terms of local transfer of heat. On the scientific side, our results have the natural side effect of “breathing life” in the large community of network scientists, opening new directions of both theoretical and experimental research. On a more practical side, by grasping the underlying mechanisms of the propagation of avalanches, we have opened the road to engineer novel materials based on abrupt transitions, paving the way to the creation of new *highly-sensitive* sensors.

An example for such a sensor could be the *single photon detector*. Utilizing a system of interdependent superconducting networks can create the situation that a collision of a single photon on a random link of the network would generate heat that destroys the link by exceeding its critical temperature. This leads to a cascade of failures resulting in abrupt transition of the entire system, thus giving rise to an extremely sensitive and effective sensor.

3 Experimental

In order to fabricate a real-world physical system of interdependent superconducting networks we need a sample with three layers. The first ("bottom") and the third ("top") layer are disordered superconductor networks and the second layer is a coupling layer that must be a strong electrical insulator and reasonable thermal conductor (see Fig. 9)

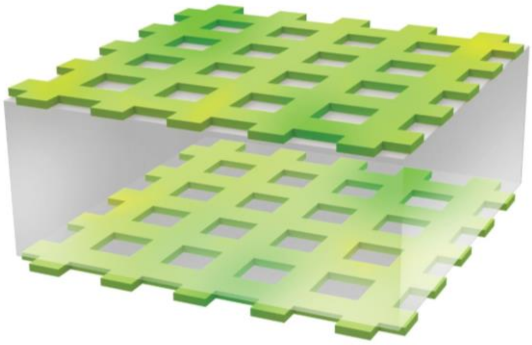

Figure 9: Sketch of our interdependent superconducting networks system. Two superconducting networks (1st and 3rd layer) are coupled by an insulating medium (2nd layer).

3.1 Substrates

Because we are dealing with thin solid-state films, we need to use a substrate. The two main properties of the substrate are important for our experiment:

1. Thermal conductivity - the heat that is generated within each network can spread also through the substrate. The thermal conductivity of the substrate is thus important for the results.
2. Electrical resistivity - the current should be allowed to flow only within each network and not through the substrate. That it's why we need to ensure that the substrate is a strong electrical insulator.

3.1.1 Si versus SiO (glass)

We used two substrates, Si and SiO_2 $(glass)$ wafers. These are chosen because both are strong insulators and have reasonable thermal conductivity. Still, there is a difference in their thermal conductivity at low temperature.

Fig. 10 shows the thermal conductivity of several materials from which we can estimate the thermal conductivity of Si at $3K$ to be ~ 200 $[\frac{w}{mK}]$ and the thermal conductivity of $glass$ at 3K to be ~ 0.2 $[\frac{w}{mK}]$.

Hence, the thermal conductivity of Si close to our base temperature is larger than that of $glass$ by 3 orders of magnitude.

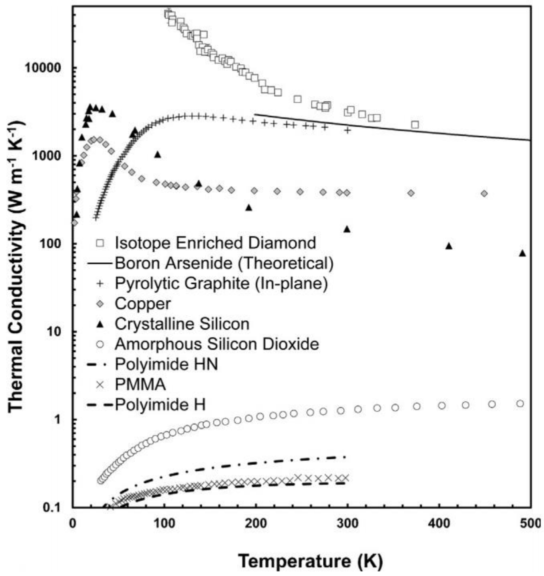

Figure 10: Thermal Conductivity vs Temperature of a number of materials [43].

3.2 Superconducting networks

We used two different superconducting materials in order to fabricate the networks and perform our experiment. The first is amorphous Indium oxide (a-InO), a disordered superconductor with wide spread of T_c and I_c and the other is Nb, a relatively ordered superconductor.

a. When high purity In_2O_3 is deposited on a substrate, an amorphous Indium Oxide (a-InO) film is formed with a certain Oxygen deficit. This oxygen deficit depends on the partial oxygen pressure in the chamber during the deposition process and controls the resistance of the sample.

b. Nb thin film is an example for relatively ordered superconductor, hence it is characterized by a narrow range of T_c.

3.3 Network geometry

Our network consists of 31X31 stripes, each stripe $4\mu m$ wide and $720\mu m$ long (Fig. 11). This structure generates 900 internal squares where each square is surrounded by 4 superconducting segments with dimension 4X20 (μm). The network was fabricated using standard photolithography and lift-off procedures utilizing the Heidelberg instruments MLA 150 machine located in the Bar-Ilan Institute of Nanotechnology & Advanced Materials (BINA center).

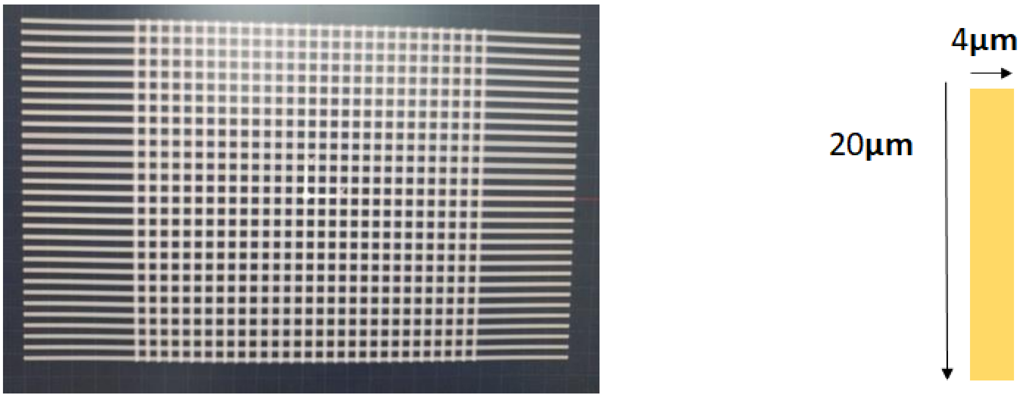

Figure 11: Left: Optical image of our network. Right: Sketch of segment in the network, each segment of the network has dimensions of 4X20 (μm).

3.4 Coupling medium

As mentioned, the medium must be a strong electrical insulator and decent thermal conductor. We chose to use Al_2O_3. Although this material is a strong insulator it has relatively large thermal conductivity, i.e $\sim 1[\frac{W}{mK}]$ at $3K$ (Fig. 12). An advantage of using Al_2O_3 is that it is relatively easy to create a pinhole free thin film.

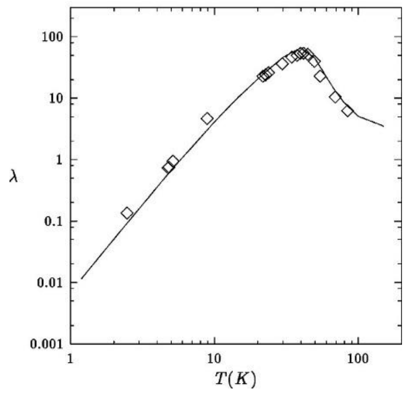

Figure 12: Thermal Conductivity in units of $[\frac{W}{cm*K}]$ vs Temperature of Al2O3 [44].

3.5 Sample preparation

The preparation of the interdependent superconducting networks model was performed using the following procedure:

1. On a substrate (Si or $glass$) we evaporated the bottom network using one of our superconducting materials.
    a. We evaporated a thin film of $50nm$ of $a\text{-}InO$ with partial oxygen pressure in the range of $60 - 80\mu Torr$. This process results in disordered superconductor with $T_c \simeq 3K$. The e-beam evaporation was done by using the evaporator in our lab.
    b. We evaporated a thin film of $50nm$ of Nb. This process results in relatively ordered superconductor with $T_c \simeq 9K$. The evaporation of the Nb performed in Dr Michael Stern lab's.
2. For the insulating medium we evaporated a thin film of $100 - 150nm$ of Al_2O_3on top of the bottom network that overlapped it fully. The evaporation was performed with high partial oxygen pressure in order to achieve a pinhole free film.

3. On top of the Al_2O_3 we evaporated a second network completely identical and overlapping the first one.
4. We fabricated two ($4nm\ Tin + 35nm\ Au$) contacts at the edges of each network in order to perform transport measurements. The contacts were written by photolithography.

Fig. 13 shows a microscopic image of our sample.

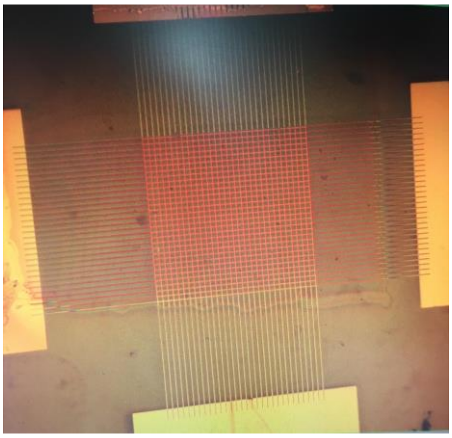

Figure 13: Microscopic image of the sample. The bottom network and the top network overlap each other and are separated by a transparent layer of insulator (Al_2O_3). The edges of each network are connected to gold contacts.

3.6 Experimental setup

In order to conduct our experiment, we used RC-102 liquid helium flow cryostat and adapted it to fit our measurement. We created a sample holder and radiation shield as seen in Fig. 14. In addition we wired the sample holder to a room temperature connector.

a) b) c) d) e)

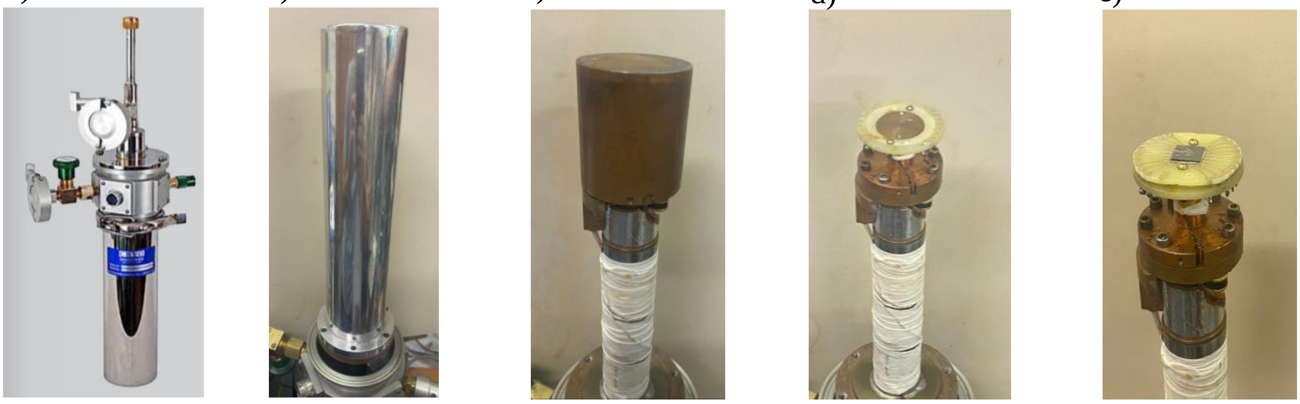

Figure 14: **a)** The RC-102, flow cryostat. **b)** The first radiation shield of the RC-102. **c)** The additional Cu radiation shield. **d)** The sample mount that was adapted to improve our thermal coupling. **e)** The sample holder connected to the sample mount.

The cryostat is cooled down by a continuous flow of liquid helium and is capable of a base temperature of $1.8K$.

3.7 Measurement process

We performed DC transport measurement using a Keithley 2410 source meter and Keithley 2000 multimeter for each network. We used LakeShore 330 to control the temperature in the system using a 25Ω heater and DT-670 thermometer that were placed inside the cryostat.

Our measurement process begins with the measurement of a single superconducting network in order to characterize its behavior near criticality. We performed transport measurements with heating-cooling cycles in the temperature range base to $10K$ for different values of current. Thus, we get a phase diagram for I_c and T_c. After classifying the single network case we continued to study an interdependent superconducting network sample.

We checked that there is no short between the networks by measuring the junction resistance between each pair of cross contacts.

The coupling between the networks is created by passing the same current within both networks simultaneously, thus generating *dependency links* based on heat-transfer. When a link in a network undergoes a metal-superconductor transition it generates heat that spreads to the other network through the medium.

We performed transport measurements for the coupled networks with heating-cooling cycles for different values of current, and generated a phase diagram for I_c and T_c.

4 Results

4.1 Single network characterization

In this subsection we describe our results for the single superconductor network. We measured more than ten samples showing similar results. We focus on four samples.

S_1 - $50nm$ Nb network on Si substrate.

S_2 - $50nm$ $a\text{-}InO$ network on Si substrate.

S_3 - $50nm$ Nb network on $glass$ substrate.

S_4 - $50nm$ $a\text{-}InO$ network on $glass$ substrate.

4.1.1 Transition width

Fig. 15 shows the $R(T)$ of S_1 and S_2 (Nb and $a\text{-}InO$ on Si substrate respectively).

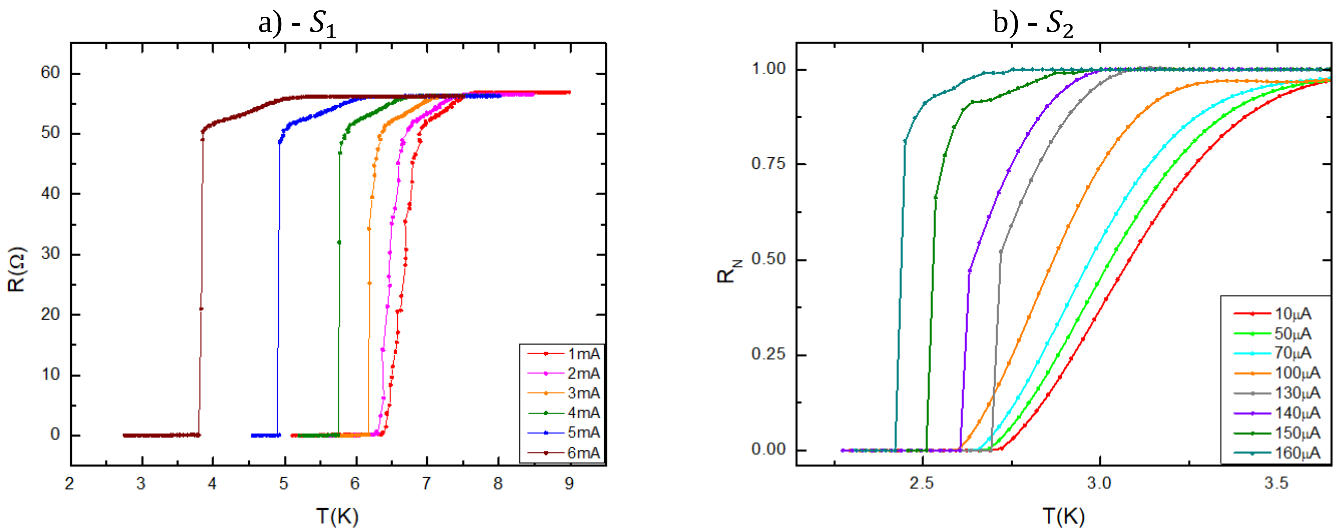

Figure 15: Resistance versus Temperature of S_1 (**a**) and S_2 (**b**) for the cooling cycle. taken at different bias currents.

It is seen that as we increase the current, the shape of the transition transits from a broad and continuous transition to a sharp and abrupt transition.

We define R_{max} to be the maximum resistance of the sample in the temperature range of base to $10K$ and the transition width to be:

$$\frac{\Delta T}{T_c} = \frac{T_2 - T_1}{T_c} \tag{1}$$

Here T_2 is the temperature at which the resistance equals $0.9R_{max}$ and T_1 is the temperature at which the resistance equals $0.1R_{max}$. T_c is defined as the temperature at which the resistance is equals $0.5R_{max}$.

Fig. 16 shows the transition width as a function of the power applied to the network given by $P = I^2R$ where I is the bias current and R is the resistance of the sample at $10K$ (this resistance does not change much for $T > T_c$).

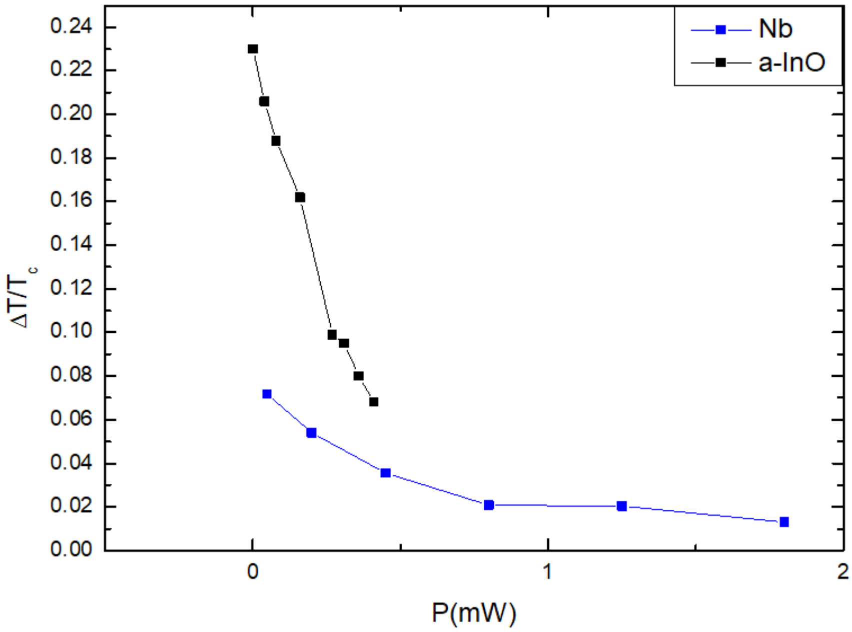

Figure 16: $\Delta T/T_c$ of S_1, S_2 as a function of power. The data points were extracted from Fig. 15.

It is seen that the transition width decreases as the power on the network is increased. In addition, the transition width of Nb is smaller than that of a-InO, hence its transition is sharper.

4.1.2 Width of hysteresis

Fig. 17 shows the $R(T)$ of samples S_3 and S_4 (Nb and $a\text{-}InO$ on a $glass$ substrate respectively), for both cooling and heating cycles.

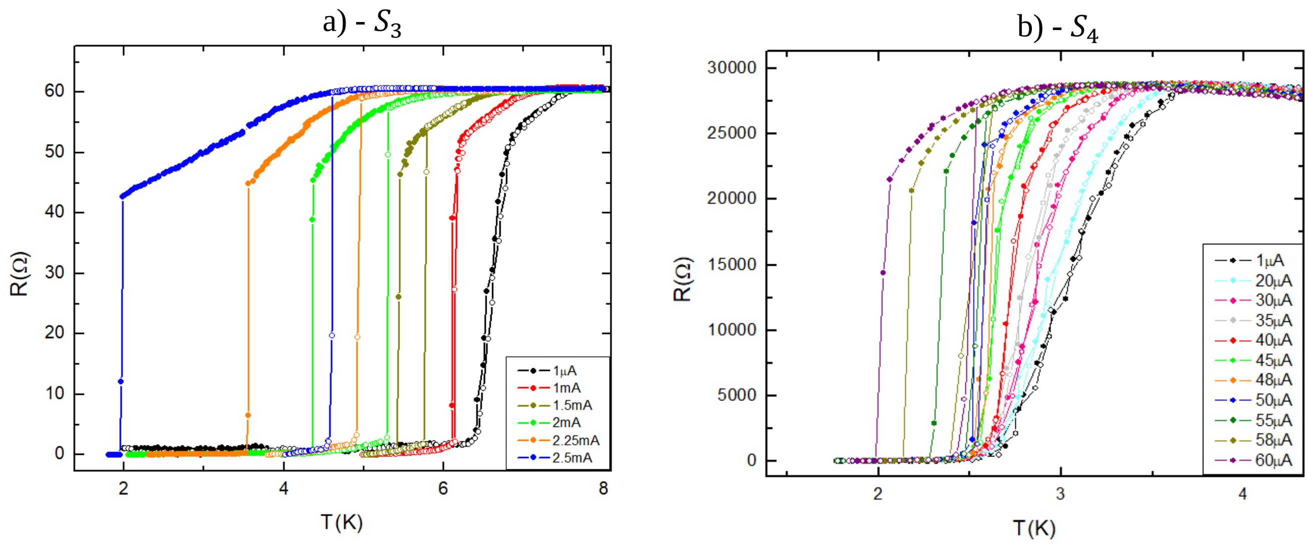

Figure 17: Resistance versus Temperature of S_3 (**a**) and S_4 (**b**) for both cooling and heating cycles. Empty circles describe the heating direction while full circles describe the cooling direction. taken at different bias currents.

Again, it is seen that increasing the current causes the transition width to increase, making the transition sharper. In addition, above a certain bias current (which is material dependent), the $R(T)$ curves exhibit hysteretic behaviour.

Fig. 18 shows the hysteresis width, defined as:

$$\Delta T_{hys} = T_{c_1} - T_{c_2} \tag{2}$$

as a function of the power on the network. Here T_{c_1} is the temperature at which the resistance equals $0.5R_{max}$ in the heating cycle and T_{c_2} is the temperature at which the resistance equals $0.5R_{max}$ in the cooling cycle.

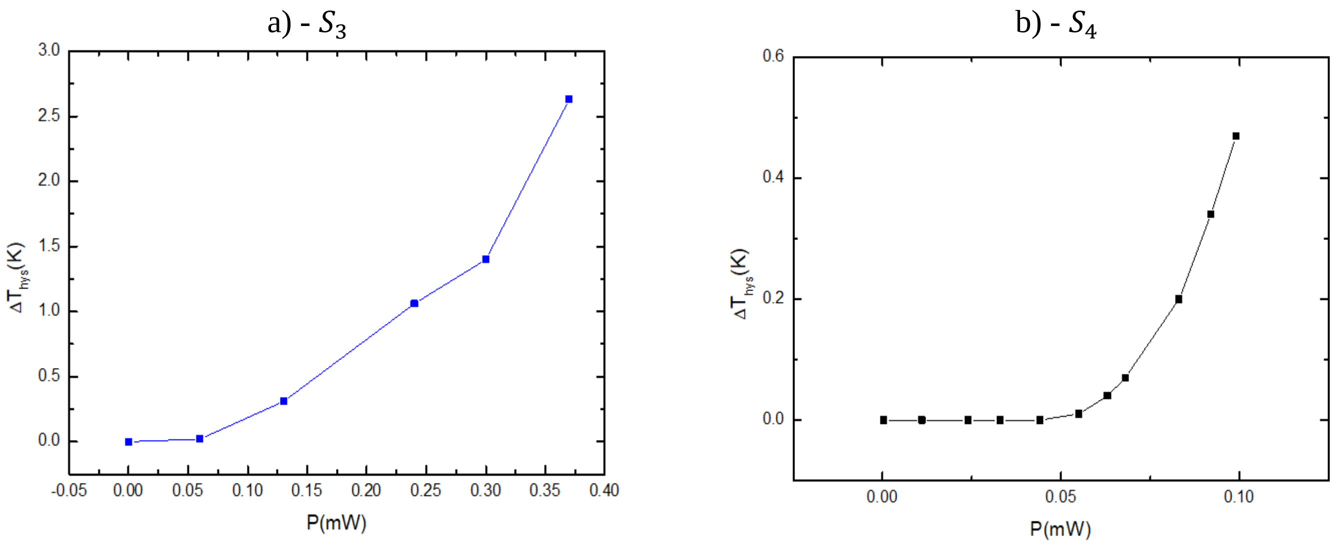

Figure 18: The hysteresis width as a function of the power for S_3 (**a**) and S_4(**b**).

It is seen that the width of the hysteresis increases as the power on the network increases.

4.1.3 Substrates comparison

Fig. 19 shows the transition width ($\Delta T/T_c$) as a function of the power on the network for S_1 and S_3 (a-InO on a Si substrate and a $glass$ substrate respectively).

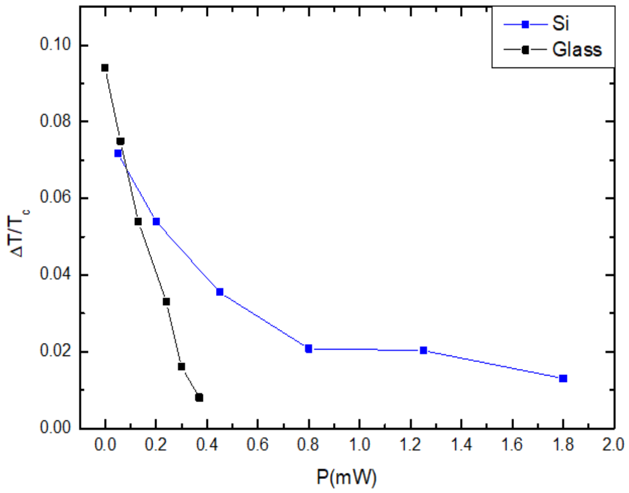

Figure 19: The transition width of S_1 and S_3. The data points were extracted from Fig. 15 b and Fig. 17 b.

These results show clearly that for $P > 0.1mW$ a glass substrate, which has lower thermal conductivity, has smaller transition width, meaning that its transition is sharper.

4.2 Coupled networks

In this subsection we describe the results of coupled networks. We focus on system of two identical networks of $a\text{-}InO$ coupled by Al_2O_3 deposited on $glass$ substrate.

We mark our networks as follows:

1. *Bottom Network* - $50nm$ $a\text{-}InO$ network on $glass$ substrate.
2. *Top Network* - $50nm$ $a\text{-}InO$ network on the Al_2O_3 coupling layer.

4.2.1 Uncoupled network behavior

We start by showing the result for each network on its own. Fig. 20 shows the $R(T)$ for the *bottom* and *top* network respectfully.

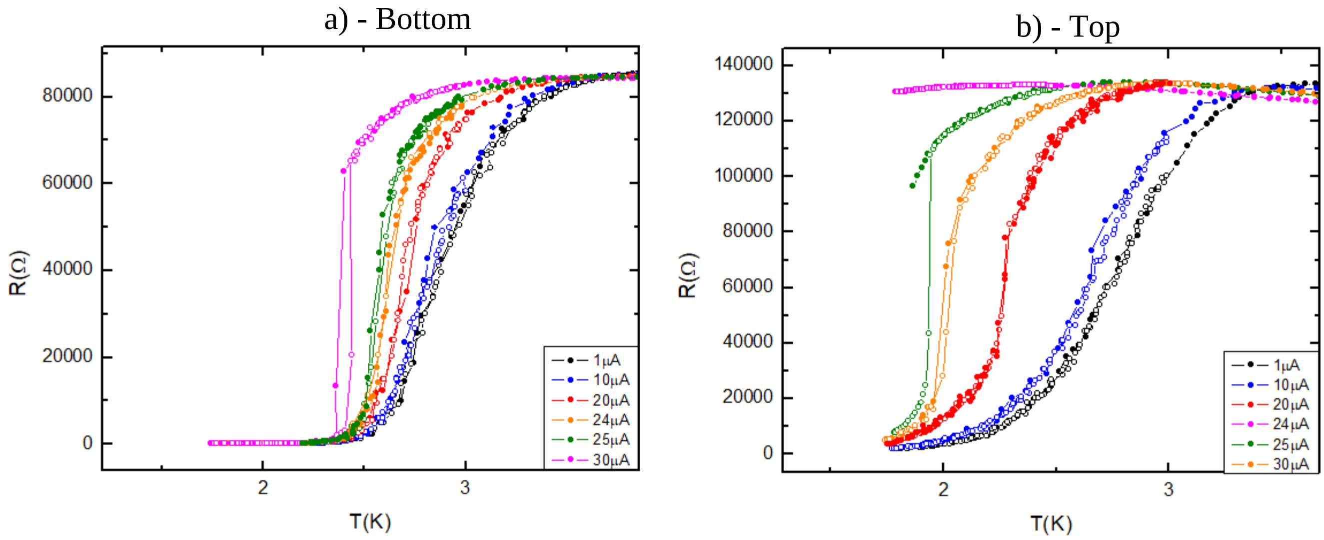

Figure 20: Resistance versus Temperature of the *bottom* (**a**) and the *top* (**b**) network for the cooling and heating cycles. Empty circles describe the heating direction while full circles describe the cooling direction. taken at different bias currents.

These results show, again, that increasing the current causes the transition width to decrease for each network on its own.

It is seen that both of the networks do not exhibit hysteretic behavior and abrupt transitions below a current of $25\mu A$, the green curve.

In order to demonstrate this, we plot the normalized $R(T)$ curves of the *top* and *bottom* network together for current of $24\mu A$ as shown in Fig. 21.

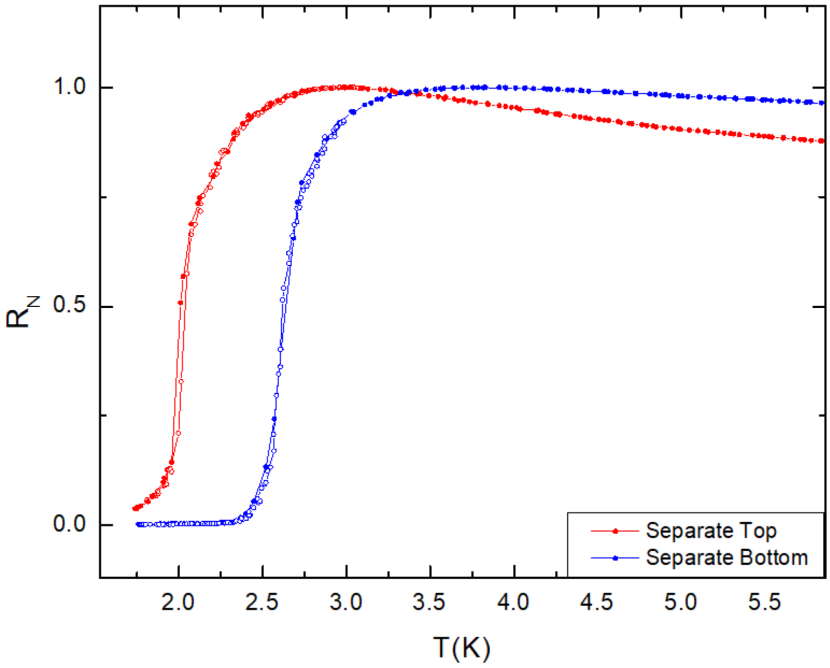

Figure 21: Normalized resistance versus temperature of the *top* (red curve) and *bottom* (blue curve) for a current of $24\mu A$. Empty circles describe the heating direction while full circles describe the cooling direction.

4.2.2 Coupled network behavior

Fig. 22 shows the $R(T)$ curves of the *top* and *bottom* network when they are coupled.

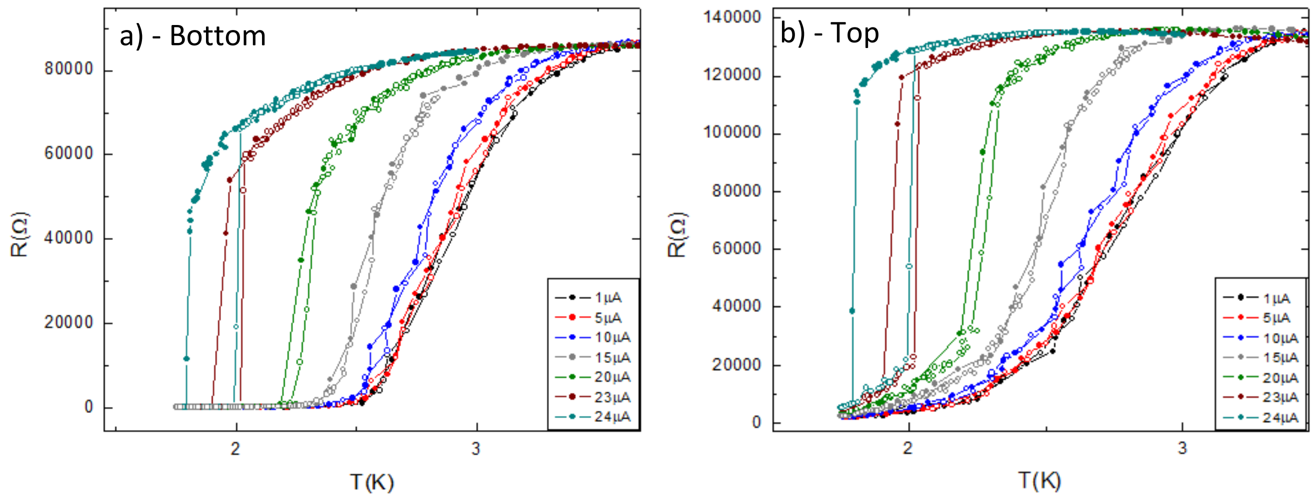

Figure 22: Resistance versus Temperature of the *bottom* (**a**) and the *top* (**b**) network for the cooling and heating cycles when they are coupled. Empty circles describe the heating direction while full circles describe the cooling direction. taken at different bias currents.

It is seen that both of the networks exhibit an abrupt transition and hysteretic behavior for currents above $20\mu A$.

Fig. 23 shows a comparison between the behavior of the coupled networks to the behavior of each network separately for current of $24\mu A$.

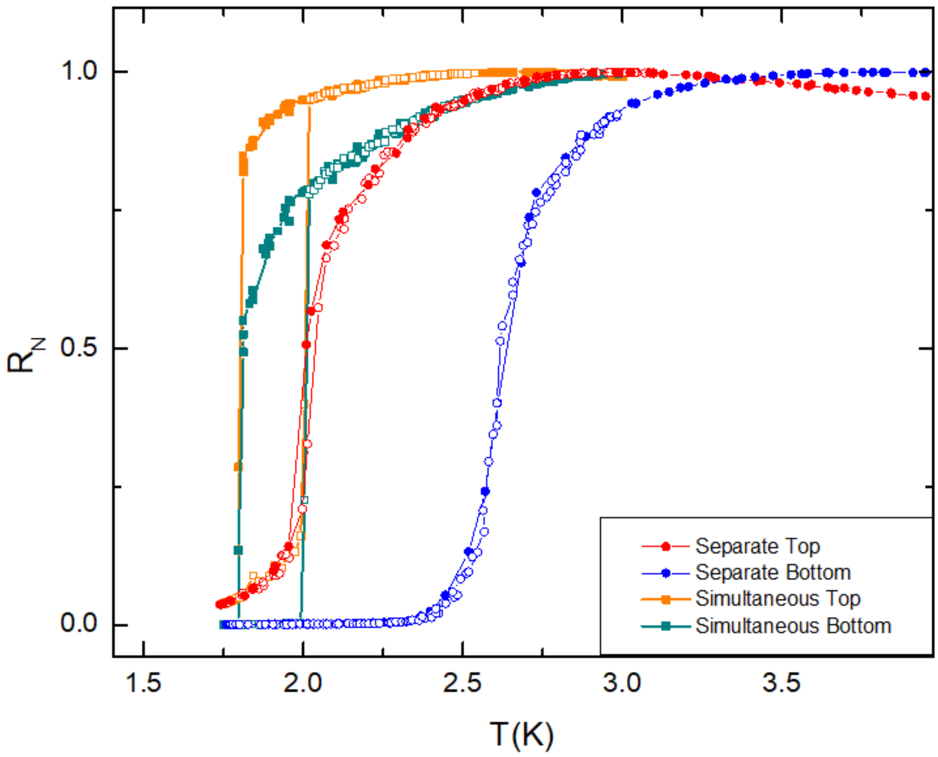

Figure 23: Normalized resistance versus temperature of the *top* (red and orange curves) and *bottom* (blue and green curves) network for a current of $24\mu A$, measured while they are coupled (orange and green squares) and in isolation (red and blue circles). Empty symbols describe the heating direction and full symbols describe the cooling direction.

Surprisingly, measuring the coupled networks shows an abrupt transition and hysteretic behavior with a shred T_c which is determined by the network with the lower transition temperature, while measuring each network separately results in a continuous transition with a unique T_c.

4.2.3 Width of hysteresis

Fig. 24 shows a comparison between the width of the hysteresis (ΔT_{hys} - Eq. 2) of the coupled networks versus that of the single network.

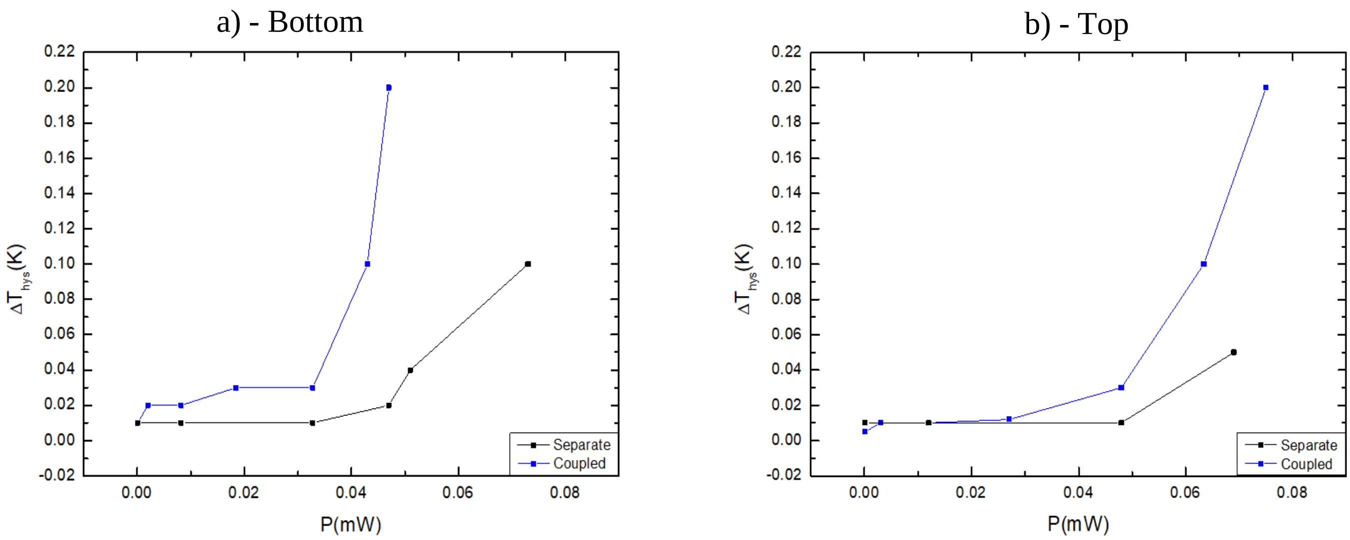

Figure 24: The comparison of width of the hysteresis of the networks while they are coupled and in isolation, for the *bottom* network (**a**) and for the *top* network (**b**). data was extracted from figs 20 and 22.

It is seen that while measured separately, each network needs more power than of the coupled case in order to exhibit a hysteretic behavior. In addition, the hysteresis width for the coupled networks is much wider for each applied power.

5 Summary and Discussion

5.1 Summary of main results

Below we summarize the main results described in the previous section.

Single network

- At low current the superconductor-insulator transition is rather broad. As the current is increased the transition becomes sharper.
- For any chosen current the Nb transition's is much sharper than that of the $a\text{-}InO$. This can be explained by the fact that the disorder of $a\text{-}Ino$ is larger, and hence has a wider spread of I_c and T_c.
- Above a certain current the $R(T)$ curves exhibit an abrupt transition and hysteretic behaviour. As the current is increased the width of the hysteresis becomes wider.
- The substrate of the sample affects the results. For a better thermal conductive substrate, a larger power has to be applied in order to observe an abrupt transition.

Coupled networks

- At low current in both networks the $R(T)$ curves exhibit broad superconductor-insulator transitions. As the current is increased the transition becomes sharper in both networks.
- Above a certain current the networks exhibit an abrupt transition with a shared T_c which is determined by the network with the lower T_c.
- For a certain current ($24\mu A$ for the sample of Fig. 25), the coupled networks exhibit an abrupt transition and hysteretic behaviour, in contrast to the continuous, non hysteretic transition which is observed for each network when it is in isolation, for the same current.
- For each chosen current, the width of the hysteresis on each coupled network is wider than the width of the hysteresis of the isolated network for the same current.

5.2 Model

To reach a theoretical understanding of the phenomena observed in the experiments we collaborated with Prof. Shlomo Havlin's group in order to develop a new iterative model based on the theory of interdependent networks that contains two different kinds of interactions:

c. *Connectivity interactions* - current that flows between nodes.
d. *Dependency interaction*s - heat that propagates between dependent nodes.

5.2.1 General idea of the model

We start by considering the transition from a broad to an abrupt superconductor-insulator transition with increasing current. For a single network this can be explained in terms of a "runaway" process. When the network is initiated at low temperature, all the nodes are in the superconductor phase. During The network heating, the temperature exceeds T_c for a few random nodes, thus turning them normal. This leads to redistribution of the current flow within the network, causing other nodes to switch to a normal metal phase. The process is repeated and eventually, it leads to an avalanche and an abrupt transition.

The "runaway" process is indeed effective in explaining the results in a single network. However, we see similar effects in a coupled network where this process is not relevant. Therefore, we suggest a new, iterative model based on interdependent networks.

We begin with analyzing the system at low temperature where all the nodes of both networks are in the superconductor phase. As the system is heated, some random nodes in at least one of the networks undergo a superconductor - metal phase transition, thus causing a dissipative current flow and heating. Due to thermal coupling, this local temperature increases and heats the superposed nodes in the other network, heating in turn an increasingly growing number of nodes. This feedback thermal process continues while developing a voltage across the network, leading to a cascade of failures and a first-order phase transition.

This process is schematically described in Fig. 25

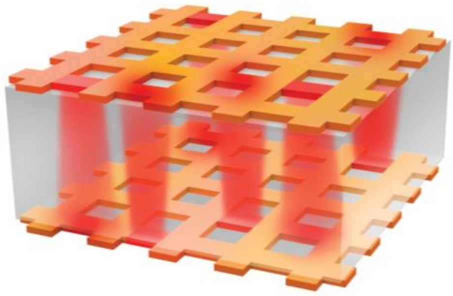

Figure 25: Sketch of the heating process of the coupled networks. The red gradient demonstrates the disorder in each network and dark red sections are in the normal phase. The current that flows within the network describes the *connectivity* links. The red beams between the networks describe the *dependency* links.

Since this model can explain the results in two coupled networks, and since the results for a single network are similar, we suggest that this model can be considered as an alternative model for each individual network as well. When all the nodes of a single network are in the superconductor phase and the system is heated, some random nodes in the network undergo a superconductor - metal phase transition, thus causing a dissipative current flow and heating. Due to heat propagation within the network, the temperature across the network increases and heats other nodes, heating in turn an increasingly growing number of nodes. This feedback thermal process can lead to a cascade of failures and a first-order phase transition.

The process of heat propagation in a single network of our network is schematically described in Fig. 26

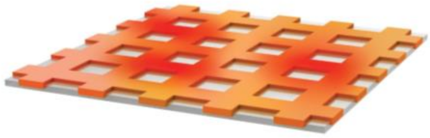

Figure 26: Sketch of the heating process of a single network. The red gradient demonstrates the disorder and dark red sections are nodes in a normal phase.

If this model is relevant, the results depend on the substrate because it also carries heat. Indeed, we see in the experiment that for a better thermal conductivity substrate a larger power has to be applied in order to observe an abrupt transition (see Fig. 21). This can be explained by the fact that for a better thermal conductive substrate, more heat is dissipated inside the substrate instead of propagating within the network, thus, less *dependency links exist* in the network.

5.2.2 Theoretical analysis

We model our network as a random array of Josephson Junctions. Where each network link is considered as a Josephson weak link. The model is iterative, each iteration in the simulation corresponds to change at the temperature of the sample in reality. After each iteration, Kirchhoff equations are resolved and the state of every junction in the network is reconsidered according to Josephson Junction characteristic as follows:

$$R^{ij} = \begin{cases} 0, & \text{(superconductor)} \\ R_0, & \text{(normal)} \\ V^{ij}/I_c^{ij}(T), & \text{(intermediate)} \end{cases} \tag{3}$$

Where $V^{i,j}$ represents the potential differences between neighboring nodes and ${I_c}^{i,j}(T)$ the critical current of the junction that can be calculated from Eq. 4.

$$ {I_c}^{i,j}(T) = {I_c}^{i,j}(0)(1 - T/{T_c}^{i,j})^2 \tag{4}$$

The critical temperature of each junction, $T_c^{i,j}$, in both networks is drawn from a Gausian distribution (with the mean value taken as the bulk T_c) that characterizes the level of disorder in the network. The critical current of each junction at zero temperature, ${I_c}^{i,j}(0)$, is obtained from the Ambegaokar–Baratoff relation:

$$ {I_c}^{i,j}(0)R_0 = \pi \Delta(0)/2e \tag{5}$$

where R_0 is the metal state resistance and $\Delta(0) = 1.76K_BT_c$ is the energy gap according to the BCS mean field formula.

After considering the state of all the junction in both networks, we evaluate the temperature of each network by considering ohmic dissipation ($P = I^2R$) within and between the networks and by the relation described in Eq. 6.

$$\begin{pmatrix} T_{eff}^A \\ T_{eff}^B \end{pmatrix} = T + \begin{pmatrix} \alpha_{AA} & \alpha_{AB} \\ \alpha_{BA} & \alpha_{BB} \end{pmatrix} \begin{pmatrix} R_A I_A^2 \\ R_B I_B^2 \end{pmatrix} \tag{6}$$

The coefficients $\alpha_{i,j}$ describe the heat conductance within and between the networks (A, B). We perform this analysis both for coupled networks and for a single network where the B components are taken to be zero. These iterations are continued until a full $R(T)$ curve is accomplished.

In order to estimate the heat conductance within a network ($\alpha_{AA} = \alpha_{BB}$) we use the following algorithm:

1. Define the reference $R(T)$ curve as the minimal current curve.
2. Look for the resistance of each $R(T)$ curve for a chosen temperature.
3. Find the appropriate temperature for this resistance in the reference curve.
4. Calculate the temperature difference $\Delta T = T_{chosen} - T_{appropriate}$ for each curve.
5. Plot $\Delta T(P)$ where P is the power applied on the network.
6. α_{AA} is estimated from the slope of $\Delta T(P)$.

Fig 27. illustrate this process for a a-InO network at $3K$.

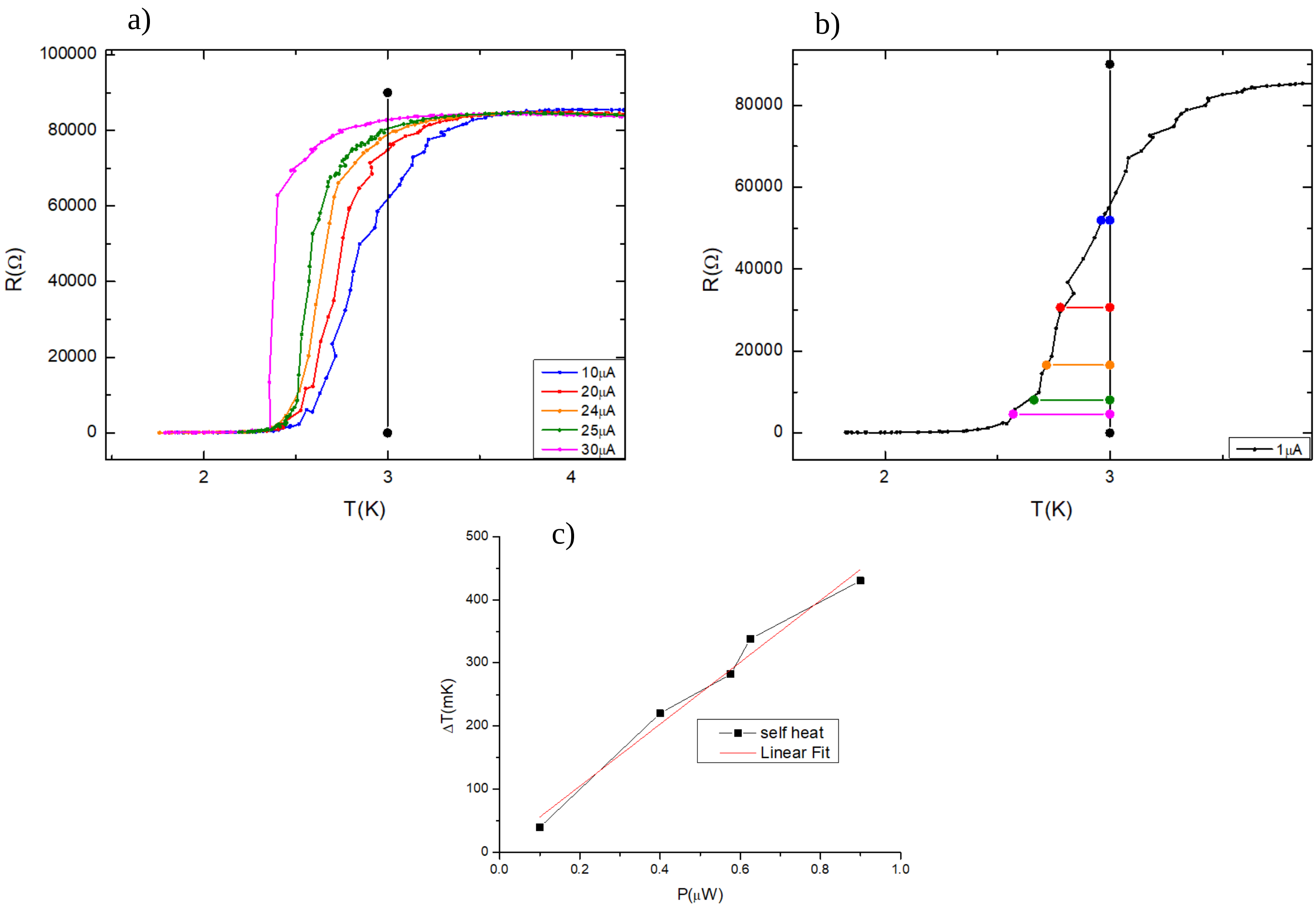

Figure 27: **a)** R(T) of an a-Ino network plotted for different currents. b**)** ΔT of each curve (color fit) compared to the reference curve. **c)** ΔT as a function of P.

We find that the relevant heat conductance within our a-InO network is $\alpha \approx 10^5[\frac{K}{W}]$. However, the distance between superposed nodes is one order of magnitude smaller compared to the distance between adjacent nodes, thus, $\alpha_{AB} = \alpha_{AB} \approx 10^6[\frac{K}{W}]$.

5.3 Comparison between experiment and theory

5.3.1 Coupled networks

Fig. 28 shows a comparison between the experiment and the simulation results for coupled networks.

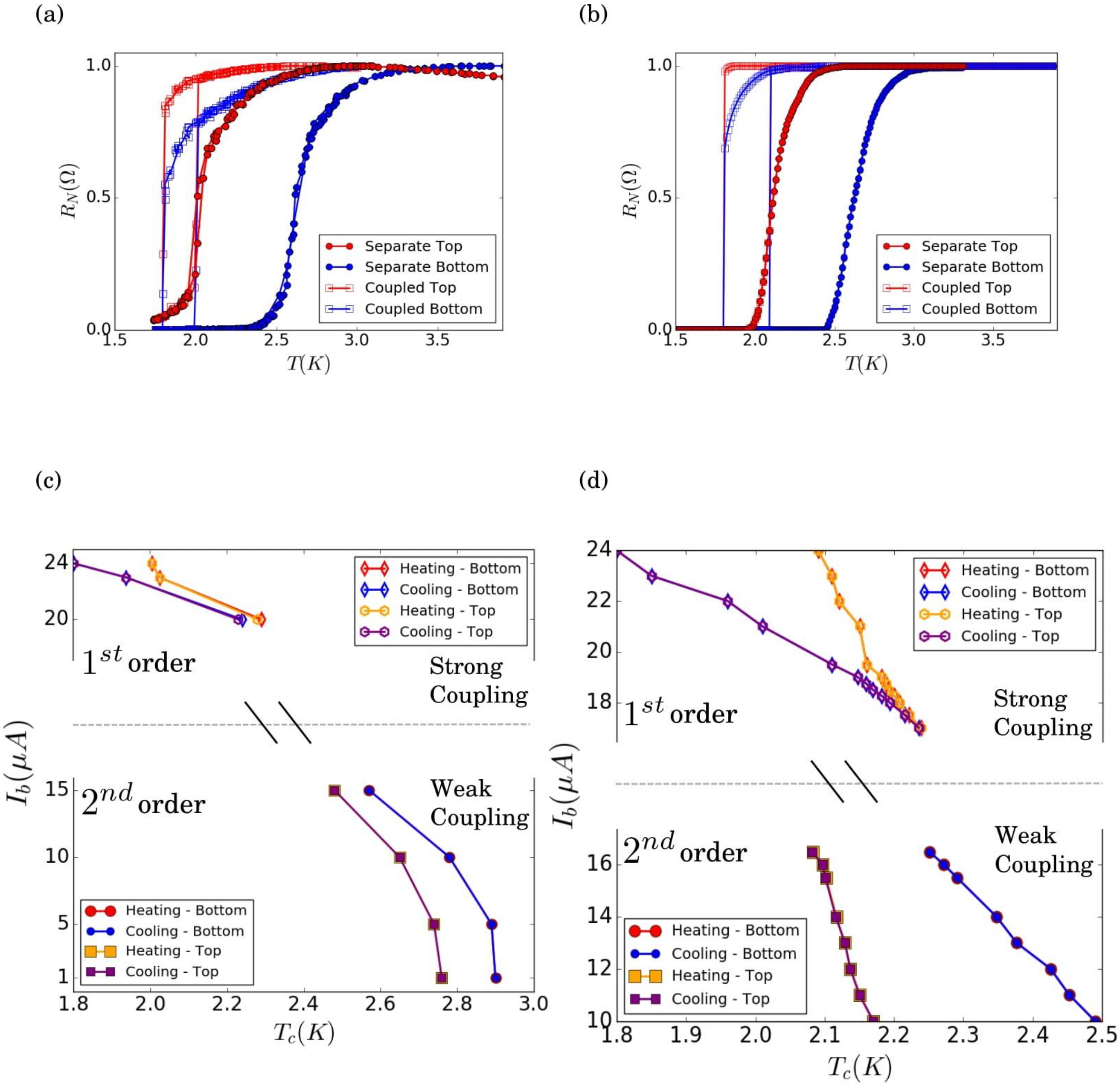

Figure 28: Normalized resistance versus temperature in experiment (**a** - taken from Fig. 23) and simulation (**b**) of the *top* (red curves) and *bottom* (blue curves) networks for a current of $24\mu A$, measured while they are coupled (squares) and in isolation (circles). The bottom panels are phase diagram, $I(T)$, of both coupled networks based on experiment (**c**) and simulations (**d**) for weak coupling (low currents - not hysteretic) and strong coupling (high currents - hysteretic). red and orange curves describe the heating cycles, blue and purple curves describe the cooling cycles. Simulations Parameters: $I_{1,c}(0) = 58\mu A$,$I_{2,c}(0) = 54\mu A$, $\alpha_{AA} = \alpha_{BB} = 5 * 10^5$ $[\frac{K}{W}]$, $\alpha_{AB} = \alpha_{BA} = 3 * 10^6$ $[\frac{K}{W}]$, $R_0 = 500\Omega$.

It is seen (a, b) both in experiment and simulation that measuring the coupled networks for current of $24\mu A$ shows an abrupt transition and hysteretic behaviour with a shred T_c, while measuring each network separately for the same current results in a continuous transition with a different T_c In each network. The shared T_c is determined by T_c of the network with the lower transition temperature. This is explained by the fact that at this temperature, some nodes in that network undergo a superconductor-metal transition. These transitions drive the process of the interdependency between the networks and finally leads to cascade and an abrupt transition.

In addition, it is seen (c, d) that for weak coupling (low currents) there is no hysteretic behavior for both networks and they behave like a single network with unique T_c. Above a certain current the networks are coupled with a shared T_c while they exhibit a hysteretic behavior.

5.3.2 Single network

Fig. 29 shows a comparison between the experiment and the simulation results for a single network.

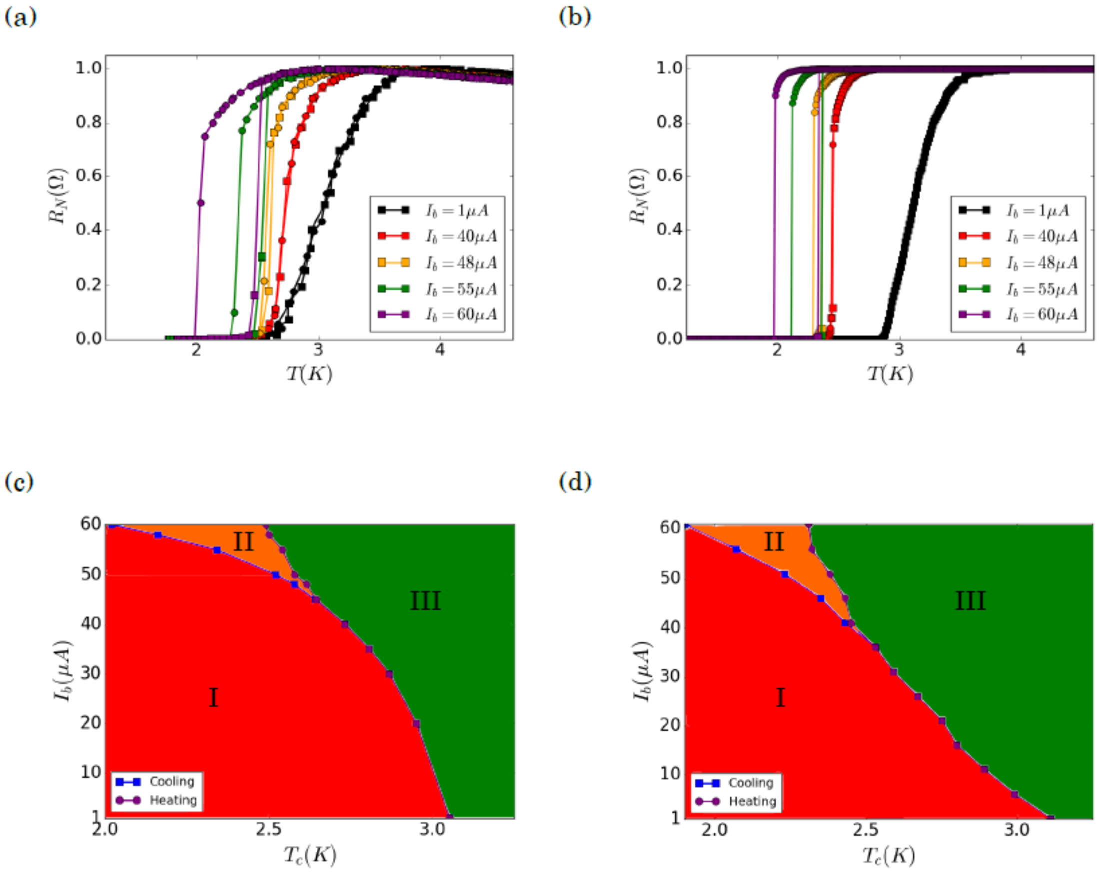

Figure 29: Normalized resistance versus temperature in experiment (**a** - taken from Fig. 19 b) and simulation (**b**) for different currents. Phase diagram, $I(T)$, based on experiment (**c**) and simulation (**d**). Blue and red curves describe cooling and heating cycles respectively. I represents the superconductor phase, III represents the normal phase and II represent the hysteretic behavior, meaning that your phase is determined according to the cycle. Simulations Parameters: $I_c(0) = 60\mu A$, $\alpha = 5 * 10^5 \; [\frac{W}{m * K}]$ and $R_0 = 500\Omega$,

It is seen (a, b) both in experiment and simulation that above a certain current, the network exhibits hysteretic behavior and an abrupt transition.

In addition, it is seen (c, d) that for low currents there is no hysteretic behavior and above a certain current a new phase appears (II phase) while hosting hysteretic behaviour and abrupt transition. In this phase, the state of the network (superconductor or normal) is determined by the cycle of the measurement, superconductor for heating cycle and normal for the cooling cycle.

5.4 Conclusions and future plans

The experiment, together with the theoretical model, show that the theory of interdependent networks can be applied in a real physical system i.e., interdependent superconducting networks. This sample is the first attempt to manifiestate and characterize the theory of interdependent networks in a real-world physical system. We believe that our experiment can also lead to new theoretical research avenues such as the application of the theory also in a single network and understanding the effect of disorder on the system (we have seen that the network with the lower transition temperature is the dominant for the model). On a more practical side, by grasping the underlying mechanisms of the propagation of avalanches, we have opened the road to engineer novel materials based on abrupt transitions, paving the way to the creation of new *highly-sensitive* sensors. An example for such a sensor could be the *single photon detector* as mentioned in the *Motivation* section.

This project focused on two coupled networks via heat layer, however, this will only be the first step. We plan to extend our study from two to more systems that include different types of interactions (for example, magnetic field). Building a physical multilayer system is indeed a fascinating perspective, which may potentially lead to the discovery of new physical properties so far overlooked, or to engineer new generations of complexity-based materials.

6 Bibliography

[1] Sergey V. Buldyrev et al. “Catastrophic cascade of failures in interdependent networks”. In: Nature 464.7291 (2010), pp. 1025–1028.

[2] Zallen, Richard. The Physics of Amorphous Solids. Blacksburg, Virgina, Wiley-Interscience, 1998. pp.137.

[3]Zallen, Richard. The Physics of Amorphous Solids. Blacksburg, Virgina, Wiley-Interscience, 1998. pp.145.

[4] Réka Albert and Albert-László Barabási. “Statistical mechanics of complex networks”. In: Rev. Mod. Phys. 74 (1 2002), pp. 47–97.

[5] Reuven Cohen et al. “Breakdown of the Internet under Intentional Attack”. In: Phys. Rev. Lett. 86 (16 2001), pp. 3682–3685.

[6] Reuven Cohen et al. “Resilience of the Internet to Random Breakdowns”. In: Phys. Rev. Lett. 85 (21 2000), pp. 4626–4628.

[7] Mark Newman. Networks: an introduction. OUP Oxford, 2010.

[8] Antonio Majdandzic et al. “Spontaneous recovery in dynamical networks”. In: Nature Physics 10.1 (2013), 34–38.

[9] Stefano Boccaletti et al. “Complex networks: Structure and dynamics”. In: Physics reports 424.4 (2006), pp. 175–308.

[10] S. N. Dorogovtsev, A. V. Goltsev, and J. F. F. Mendes. “Critical phenomena in complex networks”. In: Rev. Mod. Phys. 80 (4 2008), pp. 1275–1335.

[11] S Boccaletti et al. “The structure and dynamics of multilayer networks”. In: Physics Reports (2014). issn: 0370-1573.

[12] Ginestra Bianconi. “Interdisciplinary and physics challenges of network theory”. In: EPL (Europhysics Letters) 111.5 (2015), p. 56001.

[13] Antonios Garas. Interconnected networks. Springer, 2016.

[14] Roni Parshani, Sergey V. Buldyrev, and Shlomo Havlin. “Interdependent Networks: Reducing the Coupling Strength Leads to a Change from a First to Second Order Percolation Transition”. In: Phys. Rev. Lett. 105 (4 2010), p. 048701.

[15] Jianxi Gao et al. “Robustness of a Network of Networks”. In: Phys. Rev. Lett. 107 (19 2011), p. 195701.

[16] Jianxi Gao et al. “Networks formed from interdependent networks”. In: Nature Physics 8.1 (2012), pp. 40–48.

[17] Michael M Danziger et al. “Vulnerability of Interdependent Networks and Networks of Networks”. In: Interconnected Networks. Springer, 2016, pp. 79–99.
[18] Scott Kirkpatrick. “Classical Transport in Disordered Media: Scaling and Effective-Medium Theories”. In: Phys. Rev. Lett. 27 (25 1971), pp. 1722–1725.
[19] Scott Kirkpatrick. “Percolation and Conduction”. In: Rev. Mod. Phys. 45 (4 1973), pp. 574–588.
[20] Scott Kirkpatrick. “The geometry of the percolation threshold”. In: AIP Conference Proceedings 40.1 (1978), pp. 99–117.
[21] L. de Arcangelis, S. Redner, and A. Coniglio. “Anomalous voltage distribution of random resistor networks and a new model for the backbone at the percolation threshold”. In: Phys. Rev. B 31 (7 1985), pp. 4725–4727.
[22] D. Stauffer and A. Aharony. Introduction to Percolation Theory. Taylor & Francis, 1994.
[23] Armin Bunde and Shlomo Havlin. Fractals and disordered systems. Springer-Verlag New York, Inc., 1991.
[24] M. Barthélémy et al. “Scaling for the critical percolation backbone”. In: Phys. Rev. E 60 (2 1999), R1123–R1125.
[25] Michael M Danziger, Amir Bashan, and Shlomo Havlin. “Interdependent resistor networks with process-based dependency”. In: New Journal of Physics 17.4 (2015), p. 043046.
[26] J. Bardeen, L.N. Cooper, J.R. Schrieffer, Theory of superconductivity, Physical review, 108 (1957) 1175.
[27] P.W. Anderson, Theory of dirty superconductors, Journal of Physics and Chemistry of Solids, 11 (1959) 26-30.
[28] R. Crane, N. Armitage, A. Johansson, G. Sambandamurthy, D. Shahar, G. Grüner, Fluctuations, dissipation, and nonuniversal superfluid jumps in two-dimensional superconductors, Physical Review B, 75 (2007) 094506.
[29] D. Shahar, Z. Ovadyahu, Superconductivity near the mobility edge, Physical Review B, 46 (1992) 10917.
[30] B. Sacépé, T. Dubouchet, C. Chapelier, M. Sanquer, M. Ovadia, D. Shahar, M. Feigel’man, L. Ioffe, Localization of preformed Cooper pairs in disordered superconductors, Nature Physics, 7 (2011) 239.
[31] S. Poran, E. Shimshoni, A. Frydman, Disorder-induced superconducting ratchet effect in nanowires, Physical Review B, 84 (2011) 014529.

[32] D. Haviland, Y. Liu, A.M. Goldman, Onset of superconductivity in the twodimensional limit, Physical Review Letters, 62 (1989) 2180.
[33] C. Marrache-Kikuchi, H. Aubin, A. Pourret, K. Behnia, J. Lesueur, L. Bergé, L. Dumoulin, Thickness-tuned superconductor-insulator transitions under magnetic field in a-NbSi, Physical Review B, 78 (2008) 144520. 35
[34] T.y.I. Baturina, D.R. Islamov, J. Bentner, C. Strunk, M. Baklanov, A. Satta, Superconductivity on the localization threshold and magnetic-field-tuned superconductor-insulator transition in TiN films, Journal of Experimental and Theoretical Physics Letters, 79 (2004) 337-341.
[35] M. Strongin, R. Thompson, O. Kammerer, J. Crow, Destruction of superconductivity in disordered near-monolayer films, Physical Review B, 1 (1970) 1078.
[36] R. Dynes, A. White, J. Graybeal, J. Garno, Breakdown of eliashberg theory for two-dimensional superconductivity in the presence of disorder, Physical review letters, 57 (1986) 2195.
[37] M. Paalanen, A. Hebard, R. Ruel, Low-temperature insulating phases of uniformly disordered two-dimensional superconductors, Physical review letters, 69 (1992) 1604.
[38] A. Yazdani, A. Kapitulnik, Superconducting-insulating transition in twodimensional a-MoGe thin films, Physical review letters, 74 (1995) 3037.
[39] C. Bøttcher, F. Nichele, M. Kjaergaard, H. Suominen, J. Shabani, C. Palmstrøm, C. Marcus, Superconducting, insulating and anomalous metallic regimes in a gated twodimensional semiconductor–superconductor array, Nature Physics, 14 (2018) 1138.
[40] Z. Han, A. Allain, H. Arjmandi-Tash, K. Tikhonov, M. Feigel'Man, B. Sacépé, V. Bouchiat, Collapse of superconductivity in a hybrid tin–graphene Josephson junction array, Nature Physics, 10 (2014) 380.
[41] S. Poran, T. Nguyen-Duc, A. Auerbach, N. Dupuis, A. Frydman, O. Bourgeois, Quantum criticality at the superconductor-insulator transition revealed by specific heat measurements, Nature communications, 8 (2017) 14464.
[42] B. Sacépé, C. Chapelier, T. Baturina, V. Vinokur, M. Baklanov, M. Sanquer, Disorder-induced inhomogeneities of the superconducting state close to the superconductor-insulator transition, Physical review letters, 101 (2008) 157006.
[43] Moore, Arden L., and Li Shi. "Emerging challenges and materials for thermal management of electronics." Materials today 17.4 (2014): 163-174.
[44] Berman R. 1951The thermal conductivities of some dielectric solids at low temperatures (Experimental)Proc. R. Soc. Lond. A20890–108

תקציר

בטבע, רק לעיתים נדירות, ניתן למצוא רשתות שלא מקיימות יחסי גומלין עם רשתות אחרות ועומדות בפני עצמן. הן בדרך כלל מופיעות ביחד בתוך מערכות גדולות יותר ומשפיעות באופן לא טריוויאלי אחת על השנייה. לאור ההבנה של מציאות זו, התיאוריה של רשתות מצומדות, רשתות שבהן צומת ברשת אחת יכול להשפיע על צמתים אחרים ברשת אחרת, פותח. לאחר מאמר פורץ דרך בנושא זה [1] נאספו הוכחות מרשימות יותר לכך שמערכות של רשתות מצומדות מציגות תופעות ייחודיות הגורמות למעברים פתאומיים. דוגמה בולטת לכך היא הפסקת החשמל המפורסמת באיטליה בשנת 2003.

למרות שהתיאוריה על רשתות מצומדות נחקרת כבר למעלה מעשור, היא מעולם לא יושמה על מערכת פיזיקלית אמיתית. המחקר שלנו, הוא הניסיון הראשון לעשות זאת. על מנת לבצע זאת, צימדנו שתי רשתות מוליכי על לא מסודרים באמצעות מבודד חשמלי חזק המציג מוליכות חום סבירה. בגלל אי הסדר, לכל צומת ברשת יש טמפרטורה קריטית משלו וזרם קריטי משלו (T_c, I_c), כך אנו שולטים במצבם של צמתים ברשת. הצימוד בין הרשתות בא לידי ביטוי באמצעות העברת זרם בשתי הרשתות בו-זמנית, דבר הגורם ליצירתם של קשרים מבוססי חום בין שתי הרשתות.

במהלך המחקר, ביצענו מדידות של התנגדות אל מול טמפרטורה של שתי הרשתות בו זמנית ושל כל רשת בנפרד עבור זרמים שונים. אחת התוצאות המעניינות שקיבלנו היא שהעקומות של התנגדות אל מול טמפרטורה של שתי הרשתות המצומדות עבור זרם מסוים הציגו התנהגות היסטרטית ומעבר פאזה חד, מסדר ראשון, עם טמפרטורה קריטית משותפת, לעומת זאת, העקומה של התנגדות אל מול טמפרטורה של כל רשת בנפרד עבור אותו הזרם הציגה מעבר פאזה רציף עם טמפרטורה קריטית שונה. הטמפרטורה הקריטית המשותפת נקבעה על ידי הרשת עם טמפרטורת המעבר הנמוכה יותר.

שיתפנו פעולה ביחד עם קבוצת המחקר של פרופסור שלמה הבלין ופיתחנו תיאוריה המבוססת על רשת אקראית של צמתי ג'וזפסון המסוגלת להסביר את תוצאותינו.

אנו בטוחים שתוצאותינו הניסיוניות ביחד עם תוצאות הסימולציות של קבוצתו של פרופסור שלמה הבלין תסלולנה את הדרך להנדס מערכות פיזיקליות מצומדות שיכולות להוביל ליישומים טכנולוגיים חדישים כמו למשל, גלאים אולטרה רגישים.

עבודה זו נעשתה בהדרכתו של פרופסור אביעד פרידמן מהמחלקה לפיזיקה, אוניברסיטת בר אילן.

אוניברסיטת בר-אילן

המחלקה לפיזיקה

מעברי פאזה פתאומיים ברשתות מוליכי על מצומדות

מעיין להב

עבודה זו מוגשת כחלק מהדרישות לשם קבלת תואר מוסמך במחלקה לפיזיקה,
אוניברסיטת בר-אילן

רמת-גן, ישראל אוקטובר 2021